APPLICATION NOTE

Solar cells from chalcopyrite-type thin films analysed by electron backscatter diffraction

Introduction

Solar energy conversion is part of a long term strategy to ensure a stable and adequate supply of electrical power in the future. Photovoltaics are the only method of converting sunlight directly into electrical energy. The efficiency of a photovoltaic system is measured as the ratio of electrical power produced to the energy of the incident solar radiation. It strongly depends on the quality of the semiconducting materials used for the fabrication of solar cells. Presently, the photovoltaic market is dominated by silicon technologies, however, the challenge is to manufacture more cost effective solar cell materials and maintain a high efficiency. Most promising for the use as light absorbing materials in thin film solar cells are chalcopyrites (chemical formula $A^{I}B^{III}CV^{I}{}_{2}$) such as $CuInSe_2$, $CuGaSe_2$, and $CuInS_2$ – including solid solutions such as $Cu(In,Ga)Se_2$ [1]. These types of materials have gained enhanced importance as solar absorbers in thin-film solar cells, because they enable production of the most efficient thin film devices. An example of such a solar cell is shown in Fig. 1.

The chalcopyrite-type structure is very similar to the diamond or sphalerite (e.g., GaAs) crystal structures. Its unit cell consists essentially of two sphalerite unit cells, in which the A^{I} and B^{III} atoms are ordered on the two different cation sites, as seen in Fig. 2. The c/a ratio differs from the ideal value 2, i.e. the crystal structure is tetragonal or pseudo-cubic.

A typical chalcopyrite-type thin-film solar cell consists of a p-type, chalcopyrite-type absorber, and an *n*-type transparent window layer which together form a *p-n* junction. The window layer consists of a CdS buffer layer and a ZnO front contact. These layers with thicknesses of about 2 µm are all deposited on molybdenum-coated substrates as, e.g., glass or flexible Ti foils. The Mo layer acts as the back contact of the solar cell. A scanning electron micrograph of such a layer stack for a solar cell with $Cu(In,Ga)Se_2$ absorber is shown in Fig. 3. In addition to the layers mentioned above, a $MoSe_2$ layer is visible between Mo and $Cu(In,Ga)Se_2$, formed during the coevaporation of Cu, In, Ga, and Se.

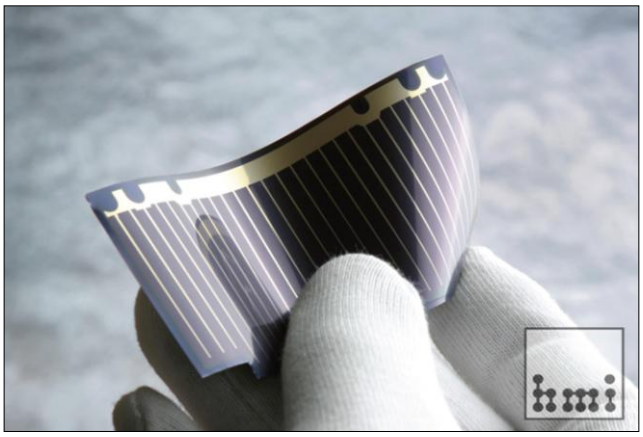

Figure 1:
Photograph of a flexible thin film solar cell on a titanium-foil substrate, based on $Cu(In,Ga)Se_2$ as light absorbing component.

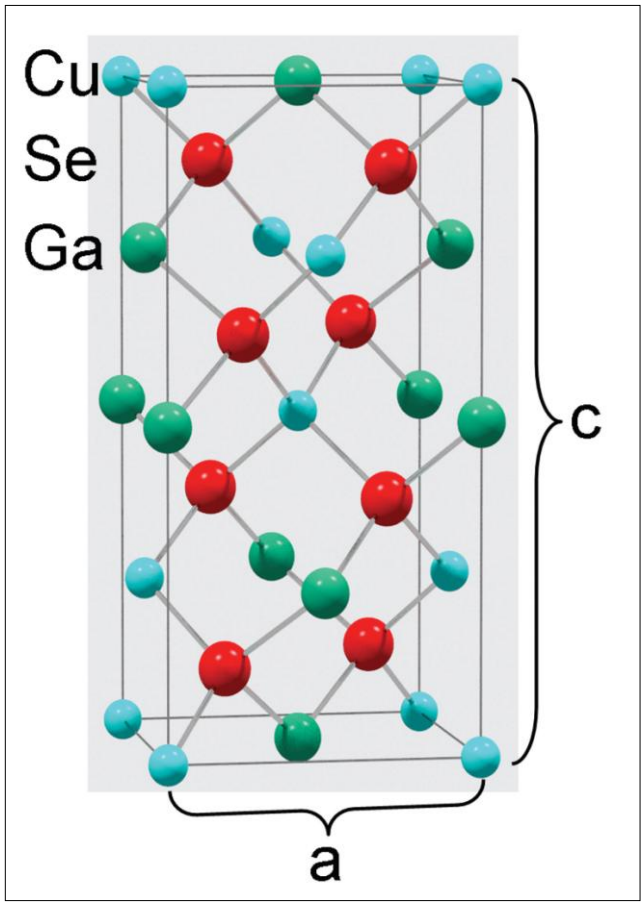

Figure 2:
Unit cell of the chalcopyrite-type $CuGaSe_2$. The lattice parameters are a=5.6Å and c=11.0Å.

Solar cells from chalcopyrite-type thin films analysed by electron backscatter diffraction

For research and development of the absorber growth, it is essential to analyse the effect of parameter variations (e.g., deposition temperature or composition) on the microstructure of the absorber and to compare this information with the solar-cell performance. Electron-backscatter diffraction (EBSD) represents a powerful technique to determine grain sizes, grain orientations and grain boundaries in polycrystalline materials, providing high precision and good statistics. The information gathered on the microstructure in the thin films is of much higher quality than that of, e.g. “apparent” grain sizes from scanning electron micrographs. Since the photocurrent in a thin-film solar cell is collected perpendicular to the surface, it is important to study the microstructure of chalcopyritetype thin films in cross-section in order to resolve possible effects of grain sizes, grain orientations and grain boundaries on the electrical properties of the solar cells.

Figure 3:
Scanning electron micrograph of a $Cu(In,Ga)Se_2$ type thin film in cross section, as well as a schematic of the solar cell and the sample geometry.

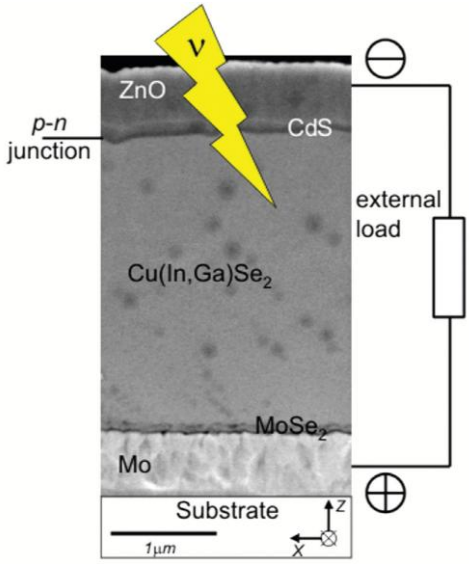

Experimental procedure

Thin-film solar cells with $CuInS_2$, $CuGaSe_2$ and $Cu(In,Ga)Se_2$ solar absorbers were produced by coevaporation [1] or sequential processing [2] on Mo-coated soda-lime glass substrates. All solar cells were completed by consecutive deposition of a CdS buffer layer, a transparent ZnO front contact and a Ni/Al contact grid.

For EBSD measurements, all samples studied were prepared by cutting thin-film solar cells into slices, forming stacks by glueing two slices face-to-face, and then carefully polishing the cross-section. Deposition of very thin (about 4-5 nm) graphite layers onto the cross-sections reduces the sample drift during the acquisitions. Scanning electron micrographs were acquired before and after the acquisition of the EBSD maps, which were used to compensate for drift in the grain size analysis. Electron backscatter diffraction pattern (EBSP) and indexing conditions were carefully chosen in order to resolve the pseudo-symmetry of the chalcopyrite-type structures, which have a c/a ratio deviating less than 1.8% from the ideal value 2 (see Table 1).

SEM type:	FEG scanning electron microscope
EBSD system:	NordlysII-S detector and Channel5 software
Accelerating voltage:	20kV
Probe current:	about 1 nA
Step size of EBSD line scans and maps:	10 to 50 nm
EBSP resolution:	2x2 binning (672 x 512 pixels)
Indexing conditions:	Advanced Fit

Table 1:
Conditions for EBSD measurements.

Solar cells from chalcopyrite-type thin films analysed by electron backscatter diffraction

Results

Texture analyses

The pole figures from EBSD line scans across a $CuGaSe_2$ layer in a completed solar cell exhibited similar texture as the results obtained by X-ray diffraction (XRD), see Fig. 4. Figs. 4a and c show the results from the EBSD line scans, which covered over 800 µm along the cross section of the thin film. Figs. 4b and d depict pole figures obtained by XRD on the same $CuGaSe_2$ sample as measured by EBSD. The pole figures show that the c-axis is parallel to the substrate surface (Figs. 4a and b). It was also found that the film shows a {110} fibre texture that is – within a deviation of about ±10° – perpendicular to the substrate surface (Figs. 4c and d).

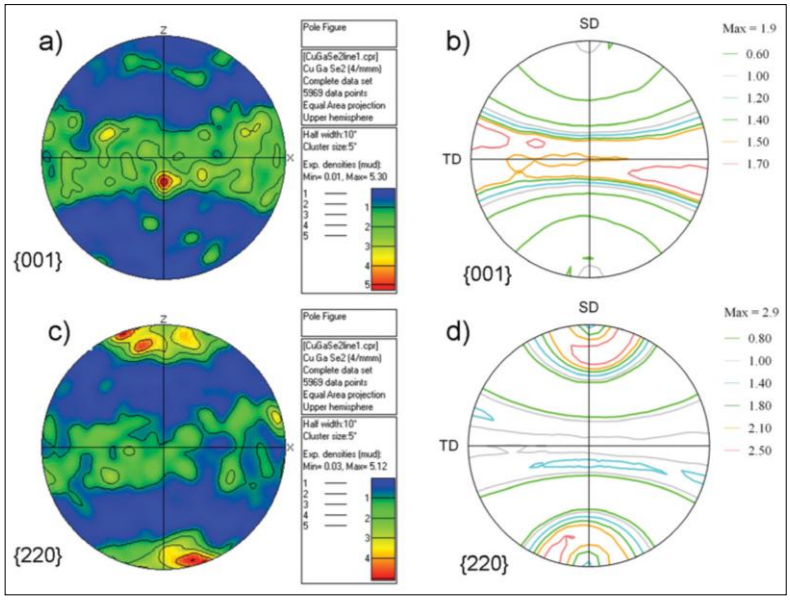

Figure 4:
Pole figures of the {001} and {220} planes, extracted from EBSD line scans (a and c) and from an XRD texture analysis (b and d), acquired on the same CuGaSe2 sample; for the sample geometry, please refer to Fig. 3. The texture data obtained by EBSD agrees well with the XRD analysis.

Orientation-distribution maps and grain boundaries

The EBSD maps shown in figure 5 were acquired using a step size of 50 nm. The microstructures of the $Cu(In,Ga)Se_2$ and $CuInS_2$ thin films are fully resolved. The grains of the $Cu(In,Ga)Se_2$ thin film appear much larger than those of $CuInS_2$.

The most frequent types of grain boundaries found in these thin films are <221>60° and <110>71° twin boundaries. Both grain-boundary types are a (near) Σ3, for this tetragonal crystal structure, where the c/a ratio is about 2 [3]. Generally, these types of grain boundaries are associated with lowest energies. The Σ3 boundaries are shown for the $Cu(In,Ga)Se_2$ and $CuInS_2$ thin films. Table 2 summarises the statistics from larger maps as those shown in Fig. 5. All the thin films contain a high percentage of Σ3 boundaries with respect to the total number of high angle boundaries.

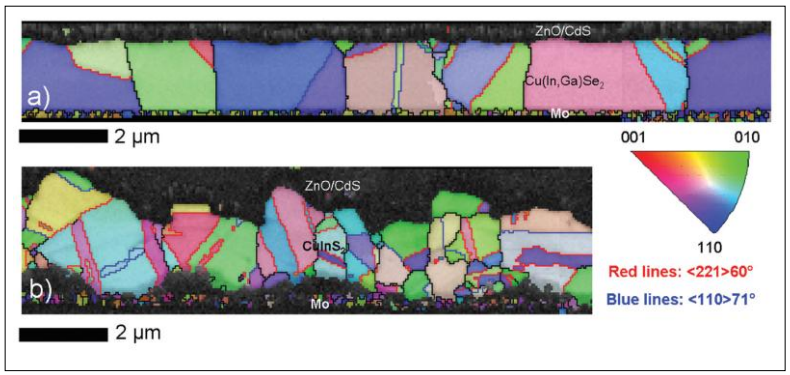

Figure 5:
EBSD maps from $Cu(In,Ga)Se_2$ (a) and $CuInS_2$ (b) thin films. The colours correspond to various crystallographic directions given by the legend, indicating the local orientations of the $Cu(In,Ga)Se_2$ and $CuInS_2$ thin films. The boundaries are highlighted for high angle grain boundaries (black lines), <221>60° (red lines) and <110>71° (blue lines).

Solar cells from chalcopyrite-type thin films analysed by electron backscatter diffraction

Grain-size distributions

The grain size measurements were done using sufficiently large EBSD maps to cover at least 300 grains in cross section. An example of the relative frequencies of the grain sizes and simulations for a $CuInS_2$ thin film is shown in Fig. 6. This type of grain size distribution agrees with the expected surfacecontrolled grain growth mechanisms for these thin films [4]. Table 2 summarises the various measurements from three different types of thin films. The grain size is one of the parameters that may affect directly the solar cell efficiency. Comparison of the three films shows that the $Cu(In,Ga)Se_2$ exhibits the largest average grain size (including Σ3 boundaries) and at the same time the highest solar-cell efficiency.

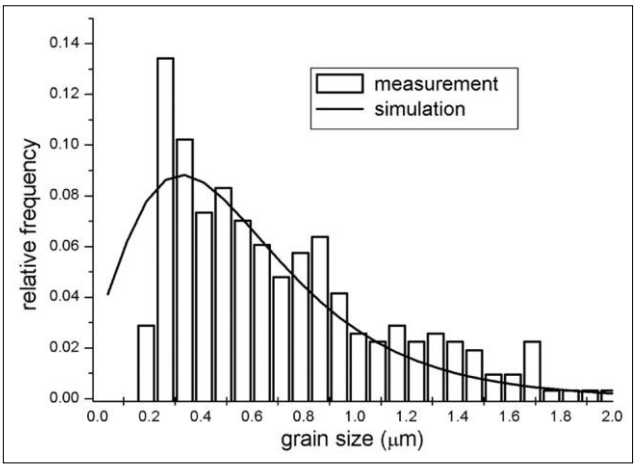

Figure 6:
Relative frequency of grain sizes (bars) and its representation by a lognormal-distribution function (solid line) for the $CuIn_2S$ sample

	Cu(In,Ga)Se2	CuInS2	CuGaSe2
Percentage of <221>60° boundaries (%)	27	27	22
Percentage of <110>71° boundaries (%)	7	17	8
Grain size excluding Σ3 boundaries (µm)	0.9	1.0	0.5
Grain size including Σ3 boundaries (µm)	0.8	0.6	0.4
Solar-cell efficiency (%)	16	10	5

Table 2:
Summary of the microstructural analyses and solar cell efficiencies for three different types of thin-film solar cells from large EBSD maps.

Solar cells from chalcopyrite-type thin films analysed by electron backscatter diffraction

Conclusion

Chalcopyrite-type thin film solar cells can be analysed successfully by means of EBSD, in spite of the difficulties given by the chalcopyrite-type, pseudo-cubic crystal structure. This is corroborated by the fact that the texture analysis by EBSD agrees well with the pole figures obtained by XRD. An additional advantage, compared to XRD measurements, is that the EBSD maps and line scans provide local orientations of the layers.

Furthermore, by means of EBSD measurements performed on cross-sections of chalcopyrite-type thin-film solar cells, a direct access to the microstructure of the thin films is provided at a relatively small effort when compared to transmission electron microscopy. The technique allows for analyses of each layer from large areas with step sizes down to 10 nm, guaranteeing good statistics and yet high spatial resolution. This microstructural information can be used to understand the influence of individual growth parameters on the solar-cell performance.

Acknowledgments

Oxford Instruments would like to thank Hahn-Meitner-Institut Berlin, Germany, in particular Dr. Daniel Abou-Ras, Melanie Nichterwitz and Dr. Christian A. Kaufmann and their colleagues for providing the EBSD data, production of the solar cells, help in sample preparation and fruitful discussions.

References

[1] C.A. Kaufmann, A. Neisser, R. Klenk, R. Scheer; Thin Solid Films 480-481 (2005) pp. 515-519.

[2] J. Klaer, R. Klenk, D. Abou-Ras, R. Scheer, H.W. Schock, D. Schmid, W. Eisele, J. Hinze, I. Luck, C.v. Klopmann, A. Meeder, U. Rühle, N. Meyer, Proceedings of the 21st European Photovoltaic Solar Energy Conference and Exhibition, Dresden, Germany, September 4-8, 2006, pp.1801-1805.

[3] H. Grimmer and M. Nespolo, Z. Kristallogr. 221 (2006) pp. 28-50.

[4] D. Abou-Ras, S. Schorr, and H.W. Schock, Grain-size distributions and grain boundaries of chalcopyrite-type thin films, submitted (2007).

This publication is the copyright of Oxford Instruments NanoAnalysis Ltd and provides outline information only which (unless agreed by the company in writing) may not be used, applied or reproduced for any purpose or form part of any order or contract or be regarded as a representation relating to the products or services concerned. Oxford Instruments acknowledges all trade marks and registrations.

visit **www.oxford-instruments.com** for more information

OXFORD INSTRUMENTS

The Business of Science®